DTU Library

Residual Stresses in SAW Welded Hollow Sections

Pedersen, Thomas Johan ; Stergiou, Alexander Spiridon Whittard ; Andreassen, Michael Joachim

Publication date:
2019

Document Version
Publisher's PDF, also known as Version of record

Residual Stresses in SAW Welded Hollow Sections

Introduction

In the offshore wind industry, welding-induced distortion and tensile residual stresses have become a major concern in relation to the structural integrity of a welded structure. These stresses have a negative impact on the integrity of the welded joint as they promote distortion, reduce fatigue life, and contribute to the stress corrosion cracking in the weld components.

Objective

This project investigates the magnitude and distribution of the welding residual stresses in offshore wind turbine foundations, called “monopiles”, which are subject to cold rolling and welding. Both processes are known to induce residual stresses with a magnitude near the yield stress. A clarification of the actual magnitudes and distributions could lead to an optimization of the fatigue design. Two 50mm thick circular hollow sections with an external diameter of 1200mm, steel grade S355NL, are used to resemble a downscaled version of a monopile foundation (Figure 1).

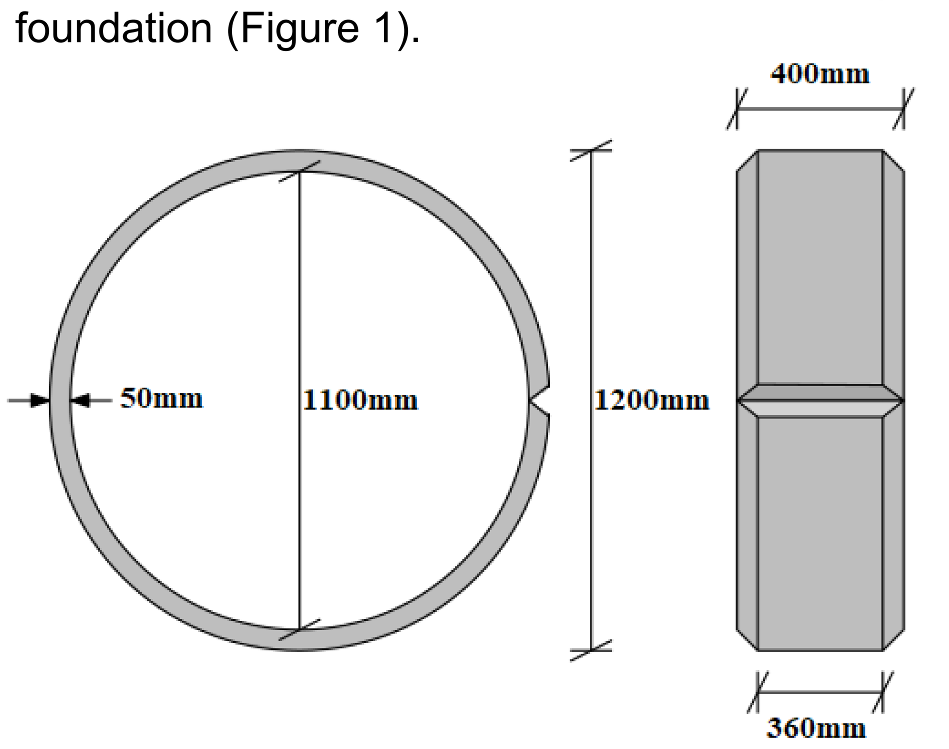

Figure 1: Hollow section dimensions

Methods

Welding

The hollow sections were welded using a Submerged Arc Welder (SAW) from ESAB. The sections were mounted on roller-beds. The welding procedure was based on a WPS from a plate. The consumables were:

- ESAB OK AUTOROD 12.22 (Wire)
- ESAB OK FLUX 10.72 (Flux)

The welding was completed with process 121 (DC 4mm) and process 123 (DC 4mm + AC TWIN 2x2.5mm)

A summary of the welding parameters are shown in Table 1, for the different passes, corresponding to the cross section of the passes in Figure 2.

Table 1: Welding pass summary

Parameters		Pass number			
		1-8	9-17	18-20	21-22
Current	DC	≤500	700	700	700
[A]	AC	-	600	-	600
Voltage	DC	≤31	31	31	31
[V]	AC	-	32	-	32
Heat-input	DC	≤1.5	4.09	2.17	4.09
[kJ/mm]	AC				

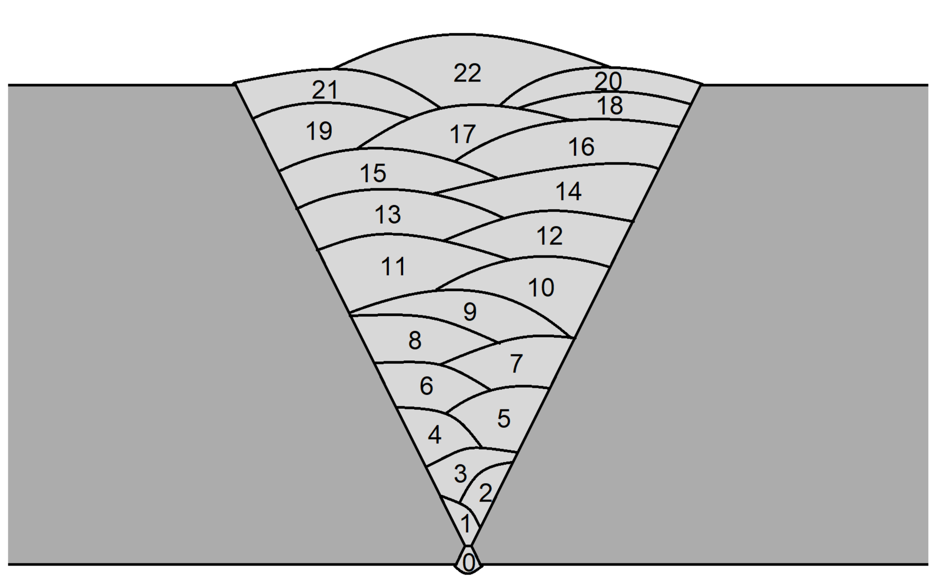

Figure 2: Weld pass positions

The stick-out was 25mm and 30mm for the DC and AC respectively. The welding speed was kept between 500-600mm/min with an interpass temperature in the range of 50-90°C.

Inspection

Table 2: Inspection summary

Non-Destructive	Destructive
DS/EN 5817:2014	DS/EN 5817:2014
Visual inspection	Slices cut from
Penetrant testing	various locations

Mechanical testing

Impact Test:
- Charpy V-testing at -50°C
- DS/EN ISO 148-1:2016

Hardness Test:
- Vickers Hardness (HV10)
- DS/EN ISO 9015-1:2011

Residual stress measurement

- Hole-drilling method
- Strain gauge: K-RY61-1.5/120R-3
- Stress Calculation: HDM & Standard ASTM E837-13: Non-Uniform

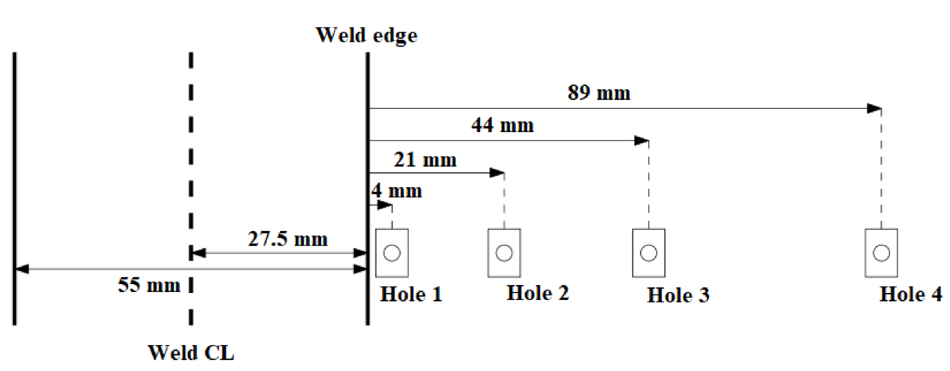

Figure 3: Positions of strain gauges

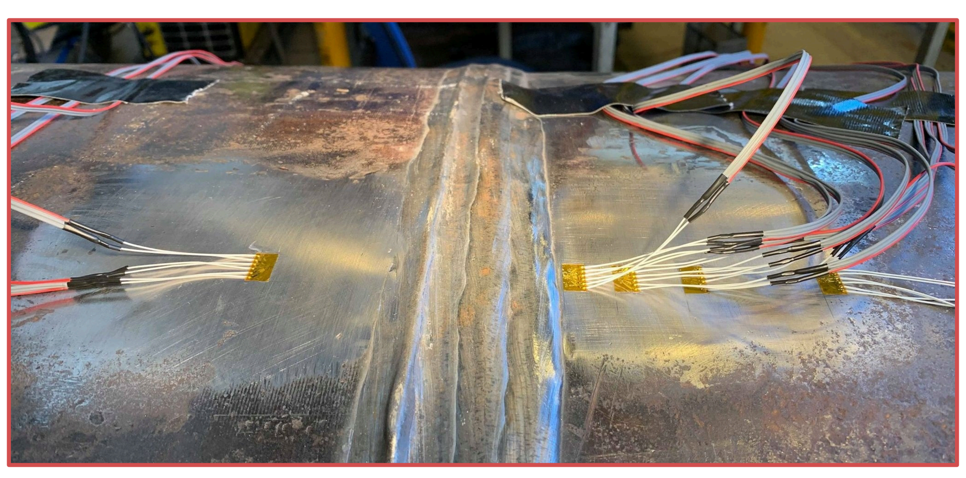

Figure 4: Strain gauges mounted on specimens

Results

Welding and Inspection

The welds indicated difficulty to weld hollow sections with the given diameter/thickness ratio. Thus, not complying to all the requirements in DS/EN ISO 5817:2014, but sufficient to fulfill the project objectives and measure the welding residual stresses.

Mechanical Testing

The results from Charpy-V testing are shown in table 3. A minimum of 16J is required according to DS/EN ISO 10025-3.

Table 3: Impact test results

Location	Nr. [-]	Energy [J]	Average [J]
VWT 0/1	1	25	21
	2	20	
	3	17	
VHT 0/1	4	31	57
	5	94	
	6	47	
VHT 2/1	7	16	19
	8	26	
	9	16	

The results from Hardness testing are shown in Table 4. The highest value of the 3 indentations in each zone is shown. The maximum allowable hardness is 380HV10 according to ISO 15614-1:2017.

Row	Parent	HAZ	Weld	HAZ	Parent
Top	183.8	315.5	195.6	310.2	189.5
Middle	187.2	267.6	216.5	206.7	194.5
Bottom	181.3	233.8	223.6	184.6	186.9

Table 4: Hardness test results

Welding residual stresses

The welding residual stresses can be seen in Figure 5 for both the longitudinal (Long) and transverse (Trans) directions.

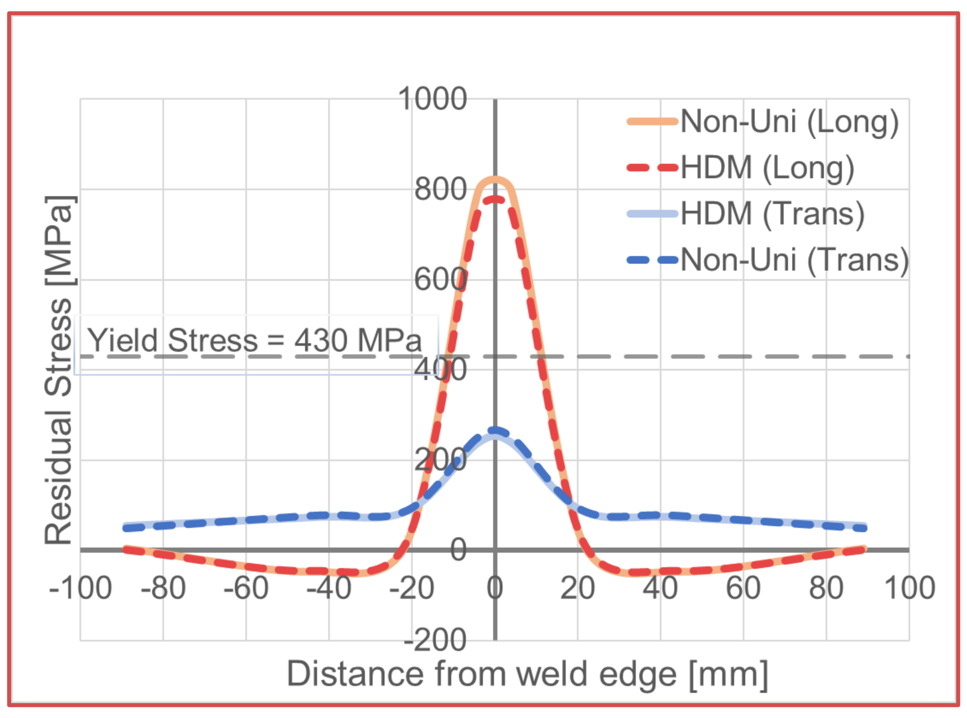

Figure 5: Residual Stress distributions

Discussion

The results from the submerged arc welding indicate difficulty welding hollow sections with the given diameter/thickness ratio.

The mechanical results showed a tendency of low impact toughness, but still passing due to an average above 16J. Low hardness values were obtained as shown in Table 4, with a maximum value of 315HV10 well below the limit of 380HV10. The low impact toughness values can be attributed to the high heat-input and low alloyed wire with a basic flux, where the low alloyed wire and basic flux result in lower hardness values.

The welding residual stresses reached 796MPa (185% of fy) and 251MPa (70% of fy) for the longitudinal and transverse directions respectively. It is well known that the hole-drilling method is only reliable for results up to approximately 80% of the yield strength, according to ASTM E837-13a. Thus, the magnitude of the longitudinal stresses cannot be concluded upon. The precision of the hole-drilling method is also influenced by the amount of weld errors. Especially excess material, weld toe and overlap could have a significant impact of the results. Due to a relatively high measurement uncertainty for welding residual stresses, it is not appropriate to directly compare specific residual stress values. However, it is possible to compare residual stress distribution trends, and determine whether the stresses are close to the yield strength.

Conclusion

- In conclusion it is challenging to produce acceptable welds when following a WPS for a plate, despite DS/EN ISO 1561-4 stating that a WPS for plates can be used for pipes with D≥500mm. A lot of factors come into play, such as geometrical imperfections, electrode placement and visibility for the welder.
- The weld passed the mechanical tests. Greater impact toughness could be achieved by lowering the heat input and increasing the alloy of the weld at the cost of the hardness.
- The hole-drilling residual stress results for the longitudinal direction can be assumed close to the yield strength. The transverse stresses reached 70% of the yield strength. The welding residual stress distribution can be seen in Figure 5.

Acknowledgements

This research activity was supported and funded by DTU Civil Engineering. The authors would like to thank DTU Civil Engineering, and the scientific and technical staff at the Technical University of Denmark for the support during the project.

DTU Civil Engineering
Department of Civil Engineering
Technical University of Denmark

Thomas Johan Pedersen
Alexander Spiridon Whittard Stergiou
Michael Joachim Andreassen
2019